AWESW2022
21st Australasian Wind Engineering Society Workshop
2 – 3 February, 2023

Aeroelastic Testing on Solar Trackers

Juan Zaracho[1], John Ginger[1], Korah Parackal[1], David Henderson[1]
[1]*Cyclone Testing Station, James Cook University, Townsville, Australia. juanignacio.zaracho@jcu.edu.au*

ABSTRACT

Ground mounted "solar trackers" that rotate about a torque tube experience dynamic effects due to wind action that can influence their structural stability eventually causing failure. This study will investigate the fluctuating wind loads on solar trackers, determine their dynamic response such as vortex excitation and torsional galloping and study the interaction of multiple arrays in a solar farm. A series of aeroelastic models will be built considering typical material and structural properties of solar trackers. These models will be tested in the wind tunnel where torque, rotational displacement and wind pressure will be measured.

1. Introduction

In recent years "solar trackers" or Single Axis Tracking (SAT) systems are increasing in popularity on solar energy generation. Solar panel modules are attached to frames that are fixed on to a horizontal axis (torque tube), allowing the system to rotate and orient towards the sun, thus increasing energy output up to 30% compared to fixed solar panel arrays. Slender components of SATs experience dynamic effects due to wind action such as vortex excitation and torsional galloping. These dynamic effects can influence their structural stability eventually causing structural failure and hence must be analysed to enable satisfactory structural design methods. Furthermore, the understanding of dynamic effects on solar trackers is limited. It is also important to study the effects (shielding, vortex-shedding induced vibrations, etc.) when wind flow interacts with a group of solar trackers arrays as is the case in solar farms.

Strobel and Banks (2014) carried out a wind tunnel model study at 1/30 and 1/50 scale on a series of long, inclined ground-mounted plates showing that vortex shedding can instigate resonance if the shedding frequency matches the natural frequency of the solar panel array structure. A study on torsional galloping conducted by Martínez-García et al (2021) demonstrated how the onset of torsional galloping is influenced by the inertia of the solar panels and the aspect ratio of the array considering the effect of the torque tube stiffness. Aeroelastic tests were carried out on seven models of the trackers, with different inertias and aspect ratios. The models were composed of up to 3 different materials to correctly reproduce their mechanical and structural characteristics. The critical velocity of torsion galloping instability was determined for a range tilt (initial inclination) and was used to produce the stability diagram. Only one isolated structure was considered, which makes them equivalent to the first-row trackers of the solar plant. It has also been found that the critical velocity is slightly higher for positive tilt angles. Valentín et al (2022) carried out a failure investigation of a solar tracker due to torsional galloping. The structure was analysed in the field and a numerical model of the structure was used to identify natural frequencies of the structure as well as the maximum stresses in the components of system. The numerical investigation confirmed that the cause of the failure was torsional galloping occurring for high-speed winds and for a tilt angle of 0°.

2. Aerodynamic effects and forces

2.1 Torsional Galloping

Torsional galloping (also torsional flutter) is a form of single degree of freedom (SDOF) aerodynamic instability in a structure, which can occur for long bodies with certain cross-sections. Consider a plate supported centrally and free to vibrate in rotation, as shown in Figure 1. Rotational velocity $\dot{\gamma}$ and moment M_t are both positive clockwise.

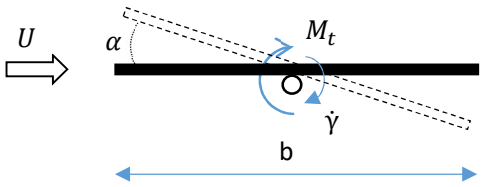

Figure 1. Diagram of a plate under torsional vibration

The motion that the structure experiences is given by the vibration equation of motion:

$$J_0\ddot{\gamma} + c_0\dot{\gamma} + k_0\gamma = M_t \tag{1}$$

Where γ is the twist angle, J_0 is the section mass moment of inertia, c_0 and k_0 are, respectively, the torsional damping and stiffness coefficients and M_t is the torsion moment. The latter is associated to a moment coefficient C_M and can be defined as:

$$M_t = \frac{1}{2}\rho U^2 b^2 C_M \tag{2}$$

Where ρ is the density of air, and b is a characteristic length (breadth or chord length). The acting moment on the structure provokes its rotation changing the initial position of the plate and changing the tilt angle α, so that $\alpha = -b\dot{\gamma}/2U$. The onset of torsional galloping on a structure is linked to a specific critical wind speed U_{cr} and is defined by Blevins (1990):

$$\frac{U_{cr}}{n_\gamma b} = -\frac{8J_0(2\pi\zeta)}{\rho b^4} \Big/ \frac{\partial C_M}{\partial \alpha} \tag{3}$$

Here, n_γ is the vibration frequency on torsional motion and ζ is the critical damping ratio of the structure. The condition under which galloping would arise is defined by $\frac{\partial C_M}{\partial \alpha} < 0$.

2.2 Vortex-induced vibrations

This mechanism occurs when shedding frequency matches the natural frequency of the tracker. Chen and Fang (1996) measured the frequencies of vortex shedding from flat plates with different beveled sharp edges at tilt angles α, from 0° to 90°, and Reynolds number Re in the range $3.5\text{x}10^3$ - $3.2\text{x}10^4$. They found that Strouhal number St can be maintained at a nearly constant level (0.16) for α from 10° on, in which the flow is fully separated. Changes of Reynolds number in the range $1.1 \text{ x } 10^4$ to $3.2 \text{ x}10^4$ have no effect on St for α between 10° and 90°. This is important to consider as it allows frequencies of vortex shedding for different wind speeds to be determined. These can then be compared against natural frequencies of different types of SAT systems to evaluate the possibility of vortex-induced vibrations.

3. Methodology

3.1 Rigid model test

Wind tunnel tests were carried out on a rigid model in the 2.5m wide × 2m high × 22m long Boundary Layer Wind Tunnel at the Cyclone Testing Station, James Cook University. Characteristics of the flow in the wind tunnel are shown in Figure 2. The approach Atmospheric Boundary Layer (ABL) simulated satisfactorily matches the AS/NZS 1170.2 (2021) terrain category 2 profile at a length scale Lr = 1/20. The velocity spectrum of the approach wind flow in Figure 1(c) compares satisfactorily with the Von-Karman spectrum at a length scale of 1/200.

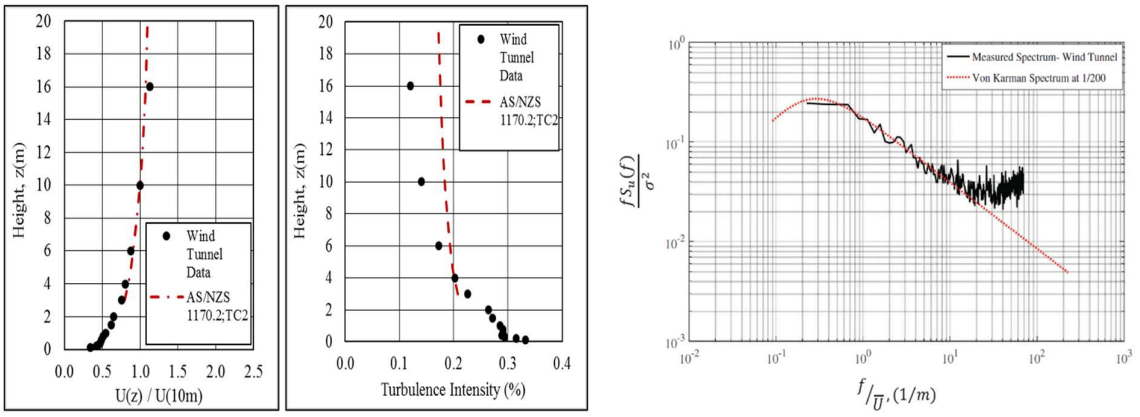

a) Mean Velocity Ratio b) Turbulence Intensity c) Turbulence spectrum.

Figure 2. Simulated approach Atmospheric Boundary Layer (ABL) flow at Length Scale of 1/20

A basic 2.5m x 5m full-scale module consisting of sixteen (i.e. 8×2) 1.2m × 0.625m solar panels were built and combined to give a six-module configuration. Each of these modules were constructed at a length scale of 1/20, giving 120mm × 250mm with a thickness of 7 mm. The module and configuration are shown in Figure 3. Pressure taps were installed on the top and bottom surfaces of the panels enabling measurement of net pressures across each panel. Tests were carried out for tilt angles α = 0°, 15°, 20°, 25°, 30°, at a fixed mid-height h = 94mm (1.88 m full-scale) and for wind direction θ from 0° to 180°.

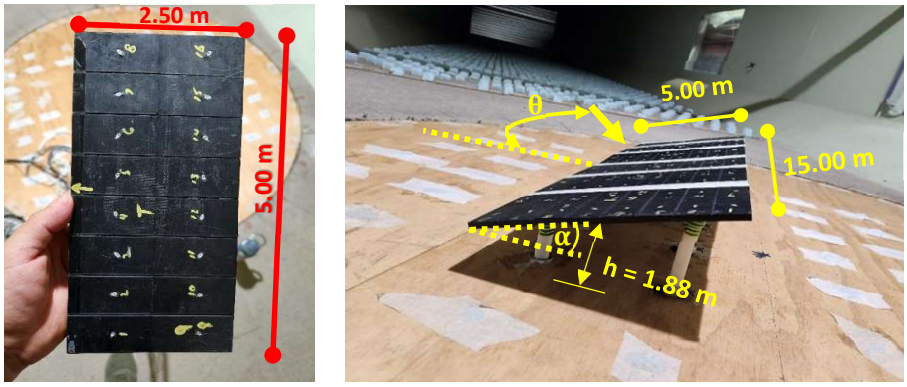

a) Solar panel module b) Six-module configuration

Figure 3. Rigid model characteristics and wind tunnel setup

As a scaling condition, St was kept equal for both the model and the full-scale structure so that, $(nL/\overline{U}_z)_m = (nL/\overline{U}_z)_p$. Following, $T_r = L_r/U_r = (1/20)/(1/3) = 3/20$ and, $T_r = T_m/T_{fs} = 3/20 = 0.15$. Hence, $T_m = 0.15 \times 10\ min \times 60\ s = 90\ s$. Top and bottom surface pressures on each model were measured simultaneously to give net (i.e. (top-bottom)) pressure fluctuations. These fluctuating pressures were sampled at 100 Hz, for 90 sec (i.e. corresponding to ~ 10 mins in full scale), and the pressure coefficients $C_p(t) = p(t)/\left(\frac{1}{2}\rho\overline{U_h}^2\right)$ recorded. Results are shown in Figure 4.

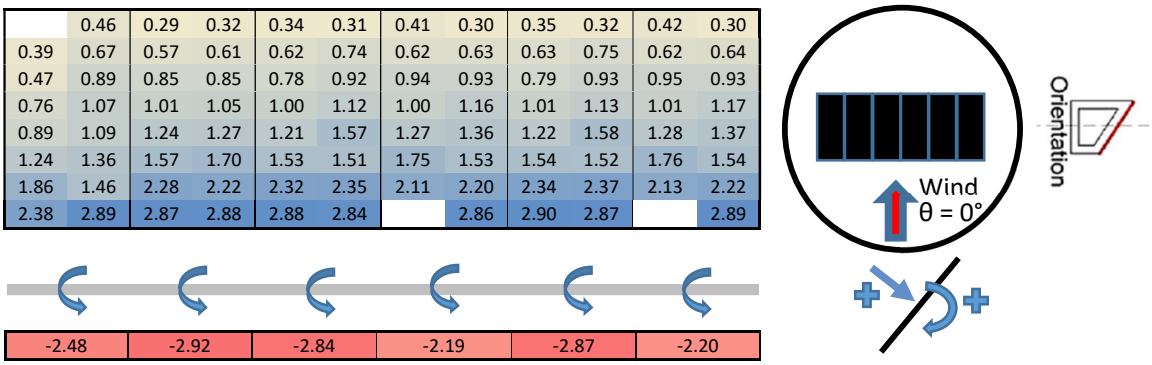

Figure 4. Pressure coefficients $\overline{Cp}$ and moment coefficients $\overline{CM}$ on six solar panel modules, α=20°, θ=0°

Results are consistent with those obtained by Kopp et al (2012), Ginger et al (2019) and others, on fixed tilt angle solar panels studies. The leading edge of the array develops high pressure which drops towards the downstream. Moment coefficients were calculated by:

$$\overline{C_M} = \sum_{i=1}^{16} C_{pn_{b_i}} \cdot b_i \Big/ b \tag{5}$$

Here, b_i is the distance from the axis at mid-height to the location of the pressure tap on the panel. For the case shown in Figure 4, the mean torque tends to be similar on all modules of the array, being slightly smaller on the laterals. The direction of the torque on each panel is given by the pressure distribution, which has a resultant located nearby the leading edge, thus generating a counterclockwise turn.

3.2 Aeroelastic Modelling

Rigid model tests can be carried out to obtain wind loading on structures, but aeroelastic models are required to evaluate the effects of aerodynamic forces. Aeroelastic modelling requires similarity of a series of non-dimensional parameters, such as: $St = nb/\overline{U}_z$; $Re = \rho\overline{U}_z b/\mu$; Density ratio = ρ_s/ρ; Froude number (Fr) $= \overline{U}_z/\sqrt{bg}$; Cauchy number (Ca) = $\rho{\overline{U}_z}^2/GJ$.

For correct scaling, or similarity in behaviour between the model (m) and the prototype (p), these non-dimensional groups should be numerically equal, or in other words, ratios between all the forces affecting the phenomena should be kept constant. In practice it is rarely possible to satisfy all these requirements and some physical understanding of the phenomena is needed to facilitate an assessment of the relative importance of the various forces so that scaling of the less significant forces may be neglected. It may also be necessary to permit the distortion of some criteria to allow a practicable model to be constructed. For instance, full-scale Re cannot be achieved in the wind tunnel. Exact maintenance of this ratio is only required when the viscous forces become of the same order of magnitude as the inertia forces. Given the sharpness of the edges of solar trackers, separation of the flow occurs at these edges and not in the boundary layer. In this case, for high Re, the flow field and hence the pressure distributions are independent of Re and so errors due to incorrect scaling are very small.

The derivation of time or velocity scales is achieved by making equal St in the model and in the full-scale structure, hence: $\left(\frac{nL}{\overline{U}}\right)_m = \left(\frac{nL}{\overline{U}}\right)_p \therefore \overline{U}_r = n_r L_r$. So, as $\overline{U}_r = L_r/T_r$, then $T_r = L_r/\overline{U}_r$. Following, if gravity forces are present, as in this study case, the time scale is constrained by the Froude number requirement, $\left(\overline{U}/\sqrt{Lg}\right)_m = \left(\overline{U}/\sqrt{Lg}\right)_p \therefore \overline{U}_r = \sqrt{L_r g_r}$, and given that $g_r = 1$ then: $\overline{U}_r = \sqrt{L_r}$ Then, $T_r = \sqrt{L_r}$. For any structure where the mode of resistance is pure torsion, the Chauchy number criterion can be modified as:

$$\left(\frac{\rho \overline{U}^2}{GJ/L^4}\right)_m = \left(\frac{\rho \overline{U}^2}{GJ/L^4}\right)_p \tag{4}$$

Where GJ is the sectional torsional rigidity. Then as the density of the air is the same for both the model and the full-scale structure, $(GJ)_r = {L_r}^4 {\overline{U}_r}^2 = {L_r}^5$. The mass distribution can be approximated considering the air density ratio is 1, and by keeping constant the inertia forces ratio so that $\rho_{s_r} = 1$. Then, if mass per unit length is considered, ${m_r} = {L_r}^2$. Therefore, setting the length scale ratio allows to obtain the other variables.

Finally, the damping ratio plays a key role in the dynamic response. For solar trackers arrays, damping in the order of 3% to 15% (Rohr et al, 2015). The adjustment of the damping ratio is challenging to control in aeroelastic models. However, damping may be modelled by using torsional springs or dashpots.

3.3 *Single array tests*

This test will be done to determine loading and dynamic response of a solar tracker for a range of tilt angles (α) and wind directions (θ). Figure 5 shows a conceptual design of the single array model, which will be built with 4 elements: the solar panel modules, the supports that will attach them to the torque tube, which will be supported by posts or pillars screwed to the ground.

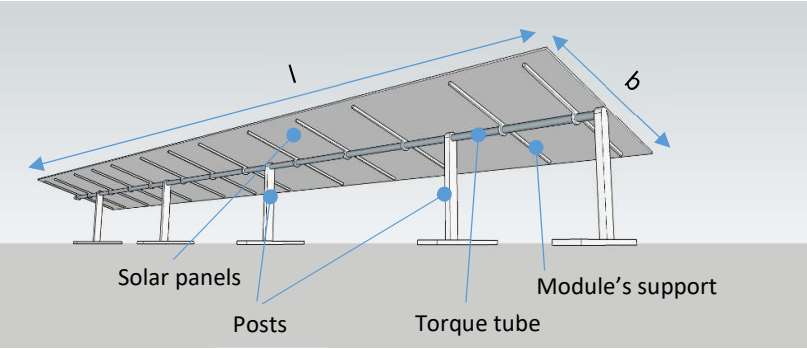

Figure 5. Single array aeroelastic model diagram

Torque M_t on the torque tube and twist angle γ on the plate will be measured. The array will be initially set at a defined tilt angle α. Wind speed will be increased progressively until the onset of torsional galloping, defining U_{cr} for each case. Torque will be measured with load cells attached to the fixed end of the torque tube. Rotational displacement γ of the plate will be video recorded with cameras oriented towards highlighted dots on the solar panels. Data collected by load cells will be used to determine the time varying torque acting on the fixed end of the torque tube. Finally, twist angle on the torque tube will be obtained by processing the video recordings with photogrammetry software.

3.4 Multi-row tests

The model built for the single array tests will be replicated to create a configuration of multiple arrays. The aim in this experiment is to obtain information on how the configuration influence the dynamic behaviour of every single row. The test will consist of varying spacing between rows as well as the initial tilt angle of each array and observing how each row responds when wind blows from different directions.

3.5 Sectional model test

A scaled section of an array will be built and tested in the wind tunnel to obtain more detail of the aerodynamic mechanism of the plate. Typical scales used for such models are 1/8 – 1/10 (Taylor and Brown, 2020). Therefore, taking advantage of this, pressure taps will be introduced in the plate, so that pressure fluctuations will be measured. Additionally, rotational displacement and torque will be measured.

4. Conclusions

Results on a rigid model test show pressure and moment distribution on solar panel arrays which vary according to wind direction and inclination of the array. A methodology to study dynamic effects using aeroelastic models of solar trackers was proposed. The models are in a conceptual design stage. The next step will require selecting non-dimensional parameters adequately as they restraint length scale and materials that can be used to build the models. Here it is valid to ask, for structures such as solar trackers, which of these parameters can be neglected to model SAT aeroelastically? Which are the most suitable length ratios? Which materials are more adequate to construct models for each case?

References

Blevins, R. D. (1990). Vibration of structures induced by fluid flow. *Harris' shock and vibration handbook, McGraw-Hill handbooks*, (part I).

Chen, Y., and Fang, C. (1996). "Strouhal numbers of inclined flat plates." Journal of Wind Engineering & Industrial Aerodynamics 61.

Ginger, J. D., Bodhinayake, G. G., and Ingham, S. (2019). "Wind loads for designing ground-mounted solar-panel arrays." Australian Journal of Structural Engineering 20(3): 204-218.

Kopp, G., Farquhar, S., and Morrison, M. (2012). "Aerodynamic mechanisms for wind loads on tilted, roof-mounted, solar arrays." Journal of Wind Engineering & Industrial Aerodynamics 111: 40-52.

Martínez-García, E., Blanco-Marigorta, E., Parrondo Gayo, J., and Navarro-Manso, A. (2021). "Influence of inertia and aspect ratio on the torsional galloping of single-axis solar trackers." Engineering Structures 243.

Rohr, C., Bourke, P. A., and Banks, D. (2015). Torsional Instability of Single Axis Solar Tracking Systems. 14th International Conference on Wind Engineering. Porto Alegre - Brazil.

Standards Australia. (2021). Structural design actions. Part 2: Wind Actions Sydney, New South Wales, Australia, Australian/New Zealand Standard, AS-NZS 1170.2:2021.

Strobel, K., and Banks, D. (2014). "Effects of vortex shedding in arrays of long inclined flat plates and ramifications for ground-mounted photovoltaic arrays." Journal of Wind Engineering and Industrial Aerodynamics 133: 146-149.

Valentín, D., Valero, C., Egusquiza, M., and Presas, A. (2022). "Failure investigation of a solar tracker due to wind-induced torsional galloping." Engineering Failure Analysis 135.